

THERMAL PROPERTIES OF TETRABUTYLLAMMONIUM BROMOTRICHLORO-, TRIBROMOCHLORO- AND TETRABROMOFERRATES(III)

D. Wyrzykowski¹, T. Maniecki², Maria Gazda³, E. Styczeń and Z. Warnke^{1*}

¹Faculty of Chemistry, University of Gdańsk, Sobieskiego 18, 80-952 Gdańsk, Poland

²Institute of General and Ecological Chemistry, Technical University of Łódź, Zwirki 36, 90-924 Łódź, Poland

³Faculty of Physics and Mathematics, Technical University of Gdańsk, Narutowicza 11/12, 80-952 Gdańsk, Poland

Thermal decomposition of tetrabutylammonium bromotrichloro-, tribromochloro- and tetrabromoferrates(III), of general formula $[(n\text{-C}_4\text{H}_9)_4\text{N}][\text{FeBr}_{4-n}\text{Cl}_n]$ ($n=0, 1, 3$), has been studied using the TG-MS, DTA, DTG as well as DSC techniques. The measurements were carried out in an argon atmosphere over the temperature range 293–1073 K. Solid products of the thermal decomposition were identified by X-ray powder diffractometry.

Keywords: tetrahalogenoferrates(III), thermal decomposition

Introduction

First members of the tetrahalogenoferrates(III), of general formula $[(\text{C}_2\text{H}_5)_4\text{N}][\text{FeBr}_{4-n}\text{Cl}_n]$ ($n=0-4$), were synthesized and characterized by FIR, Raman and Mössbauer spectroscopies in 1970 [1]. The spectroscopic [2–5], magnetic [6–8] and X-ray crystallographic [9–11] investigations revealed in these coordination entities a high-spin d⁵ iron(III) in a slightly distorted tetrahedral environment of the halogen ligands. Owing to these structural features the tetrahalogenoferrate(III) salts can serve as models for exploration of physicochemical properties of biological systems involving iron – sulfide proteins [12–13].

In recent years thermal behavior of complex compounds with transition elements has been extensively studied [14–18]. However, to the best of our knowledge, there are no reports on thermal decomposition of compounds with mixed tetrahalogenoferrate(III), $[\text{FeBr}_{4-n}\text{Cl}_n]$ ($n=0-4$), anions. Just this was the reason that prompted us to embark on these studies.

One of the previously studied compounds, $[(n\text{-C}_4\text{H}_9)_4\text{N}][\text{FeCl}_4]$, turned out to be fairly stable at elevated temperatures [19]. Its decomposition was preceded by phase transition and melting, and around 683 K iron(III) was quantitatively reduced to iron(II) both in the oxidative and inert atmospheres. In continuation of these studies, it seemed now worthwhile to learn how a gradual exchange of the chloride ligands for the bromide ones in the coordination sphere of iron(III) – in the series bromotrichloroferrate(III),

$[\text{FeBrCl}_3]^-$, tribromochloroferrate(III), $[\text{FeBr}_3\text{Cl}]^-$, and tetrabromoferate(III), $[\text{FeBr}_4]^-$ – would affect their thermal behavior. To eliminate the effect of cation on the thermal stability of the anions, all of them were stabilized by a tetrabutylammonium cation. In this contribution, thermal characteristics (TG-MS, DTA, DTG and DSC) of the bromotrichloro-, tribromochloro- and tetrabromoferrates(III) have been presented.

Experimental

Synthesis and chemical analysis

The synthesis of tetrabutylammonium bromotrichloro-, tribromochloro- and tetrabromoferrates(III) was carried out using a procedure similar to that reported for the preparation of other tetrahaloferrates(III) [19]. Thus, to an ethanolic solution of FeBr_3 (or FeCl_3) a stoichiometric quantity (ca. 0.03 mol) of tetrabutylammonium chloride (or bromide) was added to afford amorphous precipitates of $[(n\text{-C}_4\text{H}_9)_4\text{N}][\text{FeBr}_3\text{Cl}]$ (or $[(n\text{-C}_4\text{H}_9)_4\text{N}][\text{FeBrCl}_3]$). The synthesis of $[(n\text{-C}_4\text{H}_9)_4\text{N}][\text{FeBr}_4]$ was carried out using a procedure similar to that described above, except that stoichiometric quantities of FeBr_3 (ca. 0.02 mol) and tetrabutylammonium bromide were used.

All the compounds were recrystallized from ethanol and dried over P_4O_{10} in a vacuum desiccator. The composition of the compounds was established on the basis of elemental analysis (C, H, N, Cl, Br and Fe).

* Author for correspondence: warnke@chem.univ.gda.pl

Methods

The TG-DTG-DTA measurements in argon (Ar 5.0) were run on a Setsys 16/18 thermal analyzer (Setaram) coupled with a Thermostar quadrupole mass spectrometer (range 293–1073 K, corundum crucible, sample mass ca. 13–18 mg, Al₂O₃ as reference, heating rate 5 K min⁻¹, flow rate of the carrier gas 15 mL min⁻¹).

The DSC measurements were carried out in a model DSC 204 NETZSCH calorimeter (range 293–423 K, Pan Al crucible, open, sample mass ca. 2, 4 and 3.55 mg for [(n-C₄H₉)₄N][FeBrCl₃], [(n-C₄H₉)₄N][FeBr₃Cl] and [(n-C₄H₉)₄N][FeBr₄], respectively, heating rate 5 K min⁻¹, flow rate 30 mL min⁻¹).

The course of the thermal analysis was broken at points corresponding to main steps of decomposition and the residues in the crucible were quickly cooled in the stream of argon. This enabled to analyze the residues at strictly pre-determined steps of decomposition. The analysis was carried out using the X-ray powder diffractometry.

The presence of crystalline phases was checked by X-ray diffraction with the use of a Philips X'Pert diffractometer system. The XRD patterns were recorded at room temperature with CuK_α radiation ($\lambda=1.540 \text{ \AA}$). Qualitative analysis of diffraction spectra was carried out with ICDD PDF database [20].

Results and discussion

Results of thermal analysis of the [(n-C₄H₉)₄N][FeBr_{4-n}Cl_n] compounds ($n=0, 1, 3$) are compiled in Table 1. From the obtained results it follows that the thermal decomposition of compounds proceeds in two main steps. The first one is rapid and comes to an end at ca. 683 K. In the DTA curve of [(n-C₄H₉)₄N][FeBr₃Cl] there are two distinct peaks

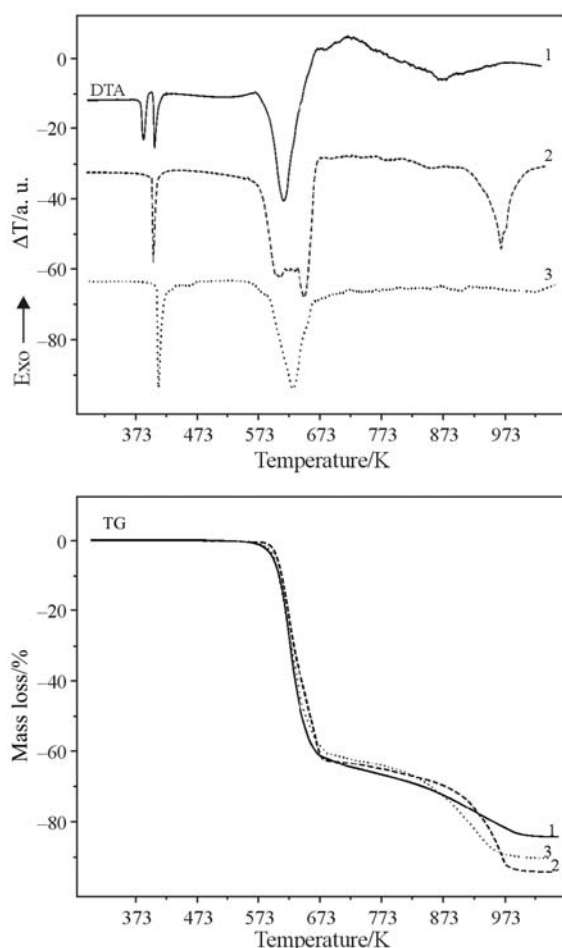


Fig. 1 TG and DTA curves of thermal decomposition of 1 – [(n-C₄H₉)₄N][FeBrCl₃], 2 – [(n-C₄H₉)₄N][FeBr₃Cl] and 3 – [(n-C₄H₉)₄N][FeBr₄] in argon

indicating two reactions to occur (Fig. 1). However, due to the rapid proceeding of these reactions, especially over the 538–683 K range, it is difficult to precisely determine temperature ranges of these reactions. The second step is much slower and terminates at ca. 1023 K.

Table 1 Thermal characteristics of [(n-C₄H₉)₄N][FeBrCl₃], [(n-C₄H₉)₄N][FeBr₃Cl] and [(n-C₄H₉)₄N][FeBr₄] in argon

Formula	Range of decomposition/K	DTG	Peak temperature ^{a)} /K			Mass loss/%	
			DTA				
			T_{σ}	T_m	T_p		
[(n-C ₄ H ₉) ₄ N][FeBrCl ₃]	528–683	613	386	403	612	62	
	683–1023	–			–	22	
[(n-C ₄ H ₉) ₄ N][FeBr ₃ Cl]	538–683	605		399	606	64	
		642			643		
	683–1023	963			967	29	
		–			–		
[(n-C ₄ H ₉) ₄ N][FeBr ₄]	543–683	626		410	629	60	
	683–1023	–			–	28	

^{a)} T_{σ} – temperature of the solid-state phase transition; T_m – melting point; T_p – peak temperature – temperature at which a maximum of the thermal effect emerges

In the DTA curves the first energetic events are seen before decomposition of the compounds (Fig. 1). With $[(n\text{-C}_4\text{H}_9)_4\text{N}]\text{[FeBr}_3\text{Cl]}$ and $[(n\text{-C}_4\text{H}_9)_4\text{N}]\text{[FeBr}_4]$ they emerge as sharp endothermic peaks assigned to melting of the compounds. With $[(n\text{-C}_4\text{H}_9)_4\text{N}]\text{[FeBrCl}_3]$, the melting is preceded by solid-state phase transition as indicated by another effect at a temperature by ca. 17° lower than the melting point. A similar behavior was noted during thermal analysis of $[(n\text{-C}_4\text{H}_9)_4\text{N}]\text{[FeCl}_4]$ [19].

Bearing in mind that all of the compounds studied here are isostructural in the solid state [21], it is interesting to note that their thermal behavior before decomposition is distinctly affected by the kind of the halogen ligands in the coordination sphere of Fe(III). This finding has gained further support from DSC analysis. Here it is also evident that the melting of the bromotrichloroferrate(III) is preceded by phase transition probably due to conversion of one polymorphic form into another (Fig. 2b). Upon cooling of $[(n\text{-C}_4\text{H}_9)_4\text{N}]\text{[FeBrCl}_3]$ down to 253 K, i.e. slightly over the phase transition point, a single exothermic peak is seen in the DSC curve (Fig. 2a). It emerges, however, at

a temperature by ca. 10° lower than that appearing upon heating. A repeated heating of the sample above its melting point, followed by cooling down to ambient temperature, results in appearance of two exothermic effects (Fig. 2b). The first one does not seem to be due to the phase transition noticed upon heating of the compound. It is rather due to supercooling of the sample due to delayed formation of the crystallization nuclei of a new phase upon recrystallization of the sample. Again, the other exothermic peak around 344 K seen upon cooling may be due to phase transition of the metastable phase to a stable one.

A similar behavior during recrystallization was noted for $[(n\text{-C}_4\text{H}_9)_4\text{N}]\text{[FeBr}_3\text{Cl]}$ (Fig. 3). There are several exothermic events upon cooling due to supercooling of the sample and formation of metastable phases.

There is another picture in the DSC plot of $[(n\text{-C}_4\text{H}_9)_4\text{N}]\text{[FeBr}_4]$. Upon first heating of the compound up to 423 K, a single endothermic peak appears assigned to its melting. Then, upon cooling from 423 down to 253 K, unlike the remaining compounds, a single exothermic peak is seen, displaced towards

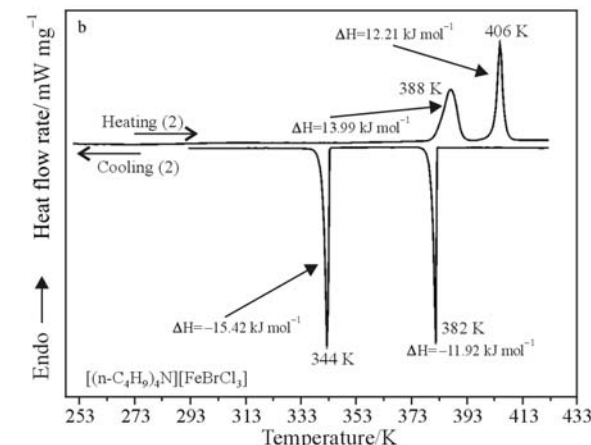
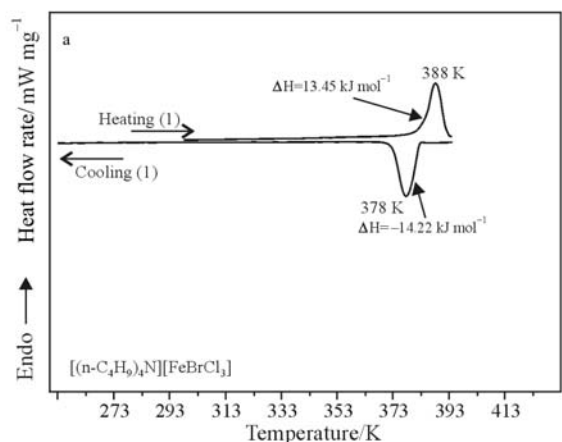


Fig. 2 A DSC plot for $[(n\text{-C}_4\text{H}_9)_4\text{N}]\text{[FeBrCl}_3]$: a – first heating and cooling; b – repeated heating and cooling

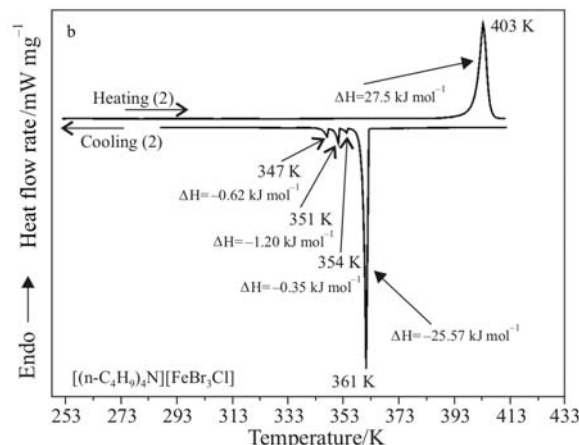
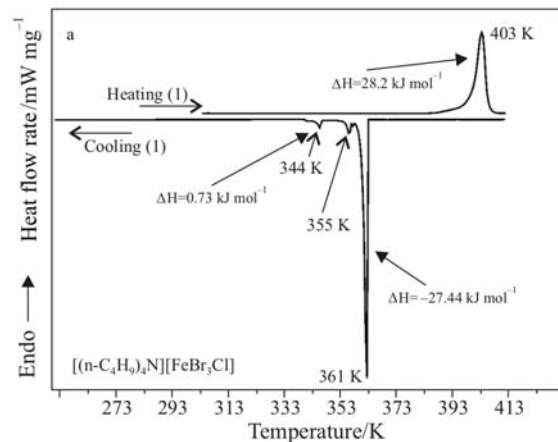


Fig. 3 A DSC plot for $[(n\text{-C}_4\text{H}_9)_4\text{N}]\text{[FeBr}_3\text{Cl]}$: a – first heating and cooling; b – repeated heating and cooling

lower temperatures probably due to supercooling of the melt (Fig. 4a). It is interesting to note that upon repeated heating of the sample up to 423 K and subsequent cooling down to ambient temperature two exothermic effects are seen (Fig. 4b). First corresponds to that emerging during the first cooling of the sample and the other appears at a temperature by ca. 8° lower. Such a thermal behavior of $[(n\text{-C}_4\text{H}_9)_4\text{N}][\text{FeBr}_4]$ is not quite clear. The additional effect may be due to conversion of the metastable phase to a stable one.

Within the series of the compounds of general formula $[(n\text{-C}_4\text{H}_9)_4\text{N}][\text{FeBr}_{4-n}\text{Cl}_n]$ ($n=0, 1, 3$) there is no distinct influence of the kind of the tetrahalogenoferrate(III) ion on both their decomposition temperatures and shapes of TG curves (Fig. 1). During the first step, both the cations and the anions undergo decomposition. Examination of the ion currents of the gaseous products, recorded during the TG-MS analysis, has shown that the halogen ligands, depending on the kind of anion, are released as $\text{C}_4\text{H}_9\text{Br}$ (m/z : 57), $\text{C}_4\text{H}_9\text{Cl}$ (m/z : 56), HBr (m/z : 80) and Cl_2 (m/z : 70, 72). Based on the previous analyses of the products of thermal decomposition of

tetrachloroferrates(III), we have found that their decomposition was non-stoichiometric [19, 22]. In addition, concurrent redox processes make any proposal for balancing the decomposition reactions difficult. A comparison of the X-ray diffraction patterns of the decomposition products of the compounds studied has shown that the largest differences between products of the first and second steps are seen when the number of the bromide ligands increases (Figs 5–7). It can thus be assumed that the coordination environment of iron in $[(n\text{-C}_4\text{H}_9)_4\text{N}][\text{FeBrCl}_3]$ present in the products of the first step is more thermally stable than the iron phases appearing in the first step products of the two remaining compounds. The mass loss during the second step (around 683–1023 K) of decomposition of $[(n\text{-C}_4\text{H}_9)_4\text{N}][\text{FeBrCl}_3]$ is mostly due to the loss of the remaining organic fragment, and an increase in temperature does not significantly affect the main form of iron present in the products of the first step.

A slightly different behavior is seen during thermal conversions of $[(n\text{-C}_4\text{H}_9)_4\text{N}][\text{FeBr}_3\text{Cl}]$ and $[(n\text{-C}_4\text{H}_9)_4\text{N}][\text{FeBr}_4]$. Here, distinct differences in the X-ray powder patterns of both steps suggest that the

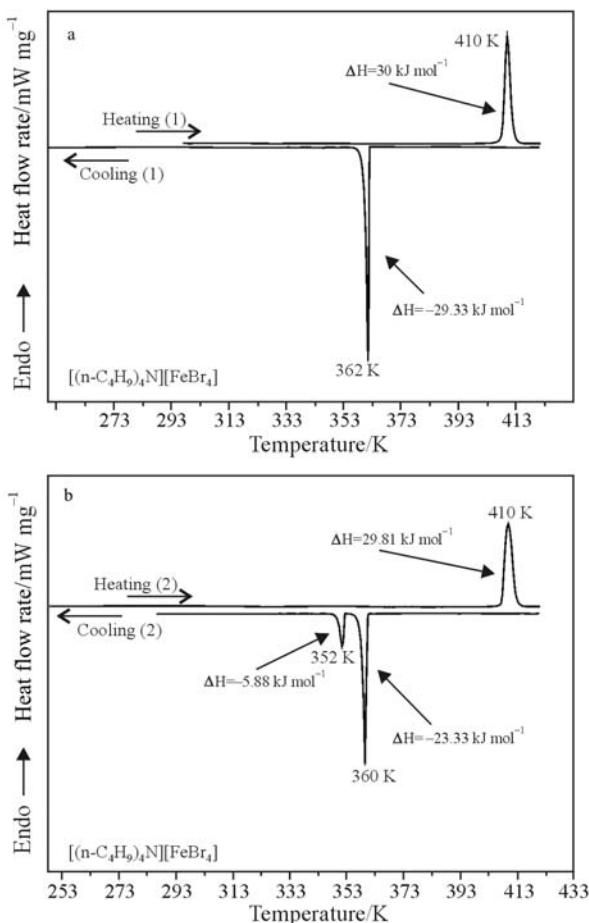


Fig. 4 DSC plot for $[(n\text{-C}_4\text{H}_9)_4\text{N}][\text{FeBr}_4]$: a – first heating and cooling; b – repeated heating and cooling

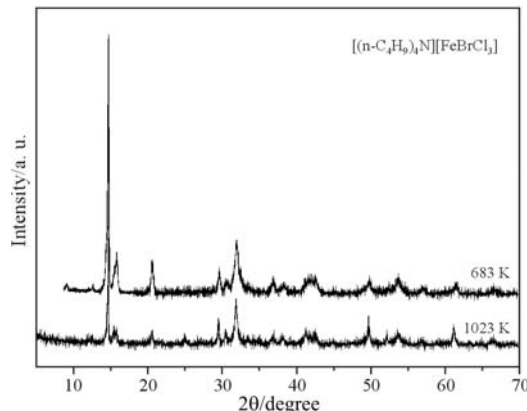


Fig. 5 Comparison of the XRPD patterns of the decomposition products of $[(n\text{-C}_4\text{H}_9)_4\text{N}][\text{FeBrCl}_3]$ in argon

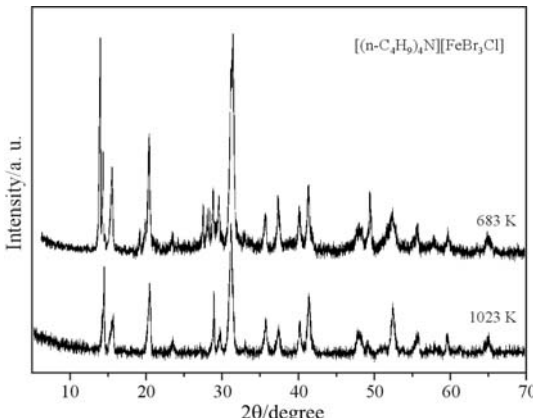


Fig. 6 Comparison of the XRPD patterns of the decomposition products of $[(n\text{-C}_4\text{H}_9)_4\text{N}][\text{FeBr}_3\text{Cl}]$ in argon

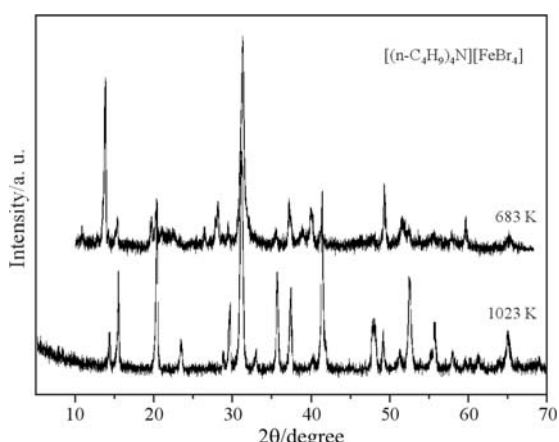


Fig. 7 Comparison of the XRPD patterns of the decomposition products of $[(n\text{-C}_4\text{H}_9)_4\text{N}][\text{FeBr}_4]$ in argon

loss in mass over the 683–1023 K range is due to the loss of the undecomposed organic matter with simultaneous conversion of the less thermally stable forms of iron in more stable ones.

Conclusions

Thermal decomposition of the compounds studied occurs in two steps. It is preceded by melting of the compounds and in the case of $[(n\text{-C}_4\text{H}_9)_4\text{N}][\text{FeBrCl}_3]$ by phase transition as well. Similar as $[(n\text{-C}_4\text{H}_9)_4\text{N}][\text{FeCl}_4]$, the compounds are fairly stable in the molten state. There is no significant influence of the kind of the tetrahalogenoferrate(III) anion on both their decomposition temperatures and shapes of TG curves. However, the number of the bromide ligands in the coordination sphere of iron(III) has a distinct influence on the composition and stability of iron species occurring in solid residues left after decomposition of the compounds. The differences due to different number of bromide ligands in the anions are seen in DSC plots. Cooling down the compounds, which previously had been heated slightly above their melting points, are accompanied by effects attributable to supercooling of the samples and formation of metastable phases that are subsequently converted to more stable ones upon further cooling. Due to non-stoichiometric progress of the decomposition reactions of the tetrahalogenoferrates(III) it is difficult to suggest equations describing their thermal degradation.

Acknowledgements

This research was supported by the Polish State Committee for Scientific Research under grant DS/8230-4-0088-6 and European Social Fund project no. ZPORR/2.22/II/2.6/ARP/U/2/05.

References

- C. A. Clausem and M. L. Good, Inorg. Chem., 9 (1970) 220.
- G. P. Bhavsar and K. Sathianandan, J. Mol. Struct., 16 (1973) 343.
- J. S. Avery, C. D. Burbridge and D. M. L. Goodgame, Spectrochim. Acta, 24A (1968) 1721.
- A. P. Ginsberg and M. B. Robin, Inorg. Chem., 2 (1963) 817.
- K. D. Butcher, S. V. Didziulis, B. Briat and E. I. Solomon, J. Am. Chem. Soc., 112 (1990) 2231.
- J. A. Zora, K. R. Seddon, P. B. Hitchcock, C. B. Lowe, D. P. Shum and R. L. Carlin, Inorg. Chem., 29 (1990) 3302.
- C. B. Lowe, R. L. Carlin, A. J. Schultz and C. K. Loong, Inorg. Chem., 29 (1990) 3308.
- Z. Warnke, R. Kruszyński, J. Kłak, A. Tomkiewicz and D. Wyrzykowski, Inorg. Chim. Acta, 359 (2006) 1582.
- D. J. Evans, A. Hills, D. L. Hughes and G. J. Leigh, Acta Crystallogr., C46 (1990) 1818.
- M. T. Hay and S. J. Geib, Acta Crystallogr., E61 (2005) m190.
- R. Kruszyński and D. Wyrzykowski, Acta Crystallogr., E62 (2006) m994.
- J. W. Lauher and J. A. Ibers, Inorg. Chem., 14 (1975) 348.
- M. C. Smith, Y. Xiao, H. Wang, S. J. George, D. Coucovanis, M. Koutmos, W. Sturhahn, E. E. Alp, J. Zhao and S. P. Cramer, Inorg. Chem., 44 (2005) 5562.
- A. Bujewski, K. Grzedzicki, J. Błżejowski and Z. Warnke, J. Therm. Anal. Cal., 33 (1988) 961.
- M. Feist, R. Kunze, D. Neubert, K. Witke and E. Kemnitz, J. Therm. Anal. Cal., 49 (1997) 635.
- S. Chen, Sh. Gao, X. Yang, R. Hu and Q. Shi, J. Therm. Anal. Cal., 73 (2003) 967.
- W. Ferenc, A. Walków-Dziewulska and P. Sadowski, J. Therm. Anal. Cal., 82 (2005) 365.
- W. Ferenc, B. Bocian and J. Sarzyński, J. Therm. Anal. Cal., 84 (2006) 377.
- D. Wyrzykowski, T. Maniecki, A. Pattek-Janczyk, J. Stanek and Z. Warnke, Thermochim. Acta, 435 (2005) 92.
- ICDD PDF-2 Database Release 1998, ISSN 1084-3116.
- D. Wyrzykowski, R. Kruszyński, U. Kucharska and Z. Warnke, Z. Anorg. Allg. Chem., 632 (2006) 624.
- D. Wyrzykowski, A. Pattek-Janczyk, T. Maniecki, K. Zaremba and Z. Warnke, Thermochim. Acta, 443 (2006) 72.

Received: September 26, 2006

Accepted: October 19, 2006

OnlineFirst: February 26, 2007

DOI: 10.1007/s10973-006-8207-9